ELSEVIER

ISPRS Journal of Photogrammetry & Remote Sensing 54 (1999) 199–214

PHOTOGRAMMETRY & REMOTE SENSING

Airborne laser scanning: basic relations and formulas

E.P. Baltsavias *

Institute of Geodesy and Photogrammetry, ETH-Hoenggerberg, CH-8093 Zurich, Switzerland

Received 17 December 1998; accepted 6 April 1999

Abstract

An overview of basic relations and formulas concerning airborne laser scanning is given. They are divided into two main parts, the first treating lasers and laser ranging, and the second one referring to airborne laser scanning. A separate discussion is devoted to the accuracy of 3D positioning and the factors influencing it. Examples are given for most relations, using typical values for ALS and assuming an airplane platform. The relations refer mostly to pulse lasers, but CW lasers are also treated. Different scan patterns, especially parallel lines, are treated. Due to the complexity of the relations, some formulas represent approximations or are based on assumptions like constant flying speed, vertical scan, etc.

Keywords: Airborne laser scanning; Terminology; Basic relations; Formulas; 3D accuracy analysis

1. Introduction

In this article, some basic relations and formulas concerning (a) laser ranging, and (b) airborne laser scanning will be given. The first group of relations explains the principle of range measurement and some factors influencing the magnitude of the received signal. The relations on airborne laser scanning are useful not just to understand some basic principles, but also for flight and project planning. They can be also used to calculate, at least approximately, unknown parameter values of ALS systems (e.g., some of the missing values in the overview given in Baltsavias, 1999, see Table 5). The last part of the paper discusses the different factors influencing the accuracy of 3D coordinates, especially ranging, positional, attitude, and time offset errors. Relations for the influence of various possible errors (attitude, scanner, ranging, position) on 3D coordinates are derived, and examples are calculated using reasonable input error values.

The formulas presented here relate mostly to pulse lasers. When they refer to continuous-wave lasers (CW lasers), this will be explicitly mentioned. The basic scan patterns on the ground are: parallel lines, meanderwise bidirectional parallel lines, bidirectional *Z*-shaped lines (or sinusoidal pattern), and elliptical scan. The first three are the most common. Some of the formulas here relate to the first scan pattern only. With some small modifications, they are valid for the other scan patterns, too. A list of used symbols with units and explanations is given in Appendix A. Symbols of equations that are not explained can be found in this Appendix.

* Tel.: +41-1-6333042; Fax: +41-1-6331101; E-mail: manos@geod.ethz.ch

0924-2716/99/$ - see front matter
PII: S0924-2716(99)00015-5

For simplicity reasons, we assume that roll and pitch angle are zero, the laser scans along a plane vertical to the flight direction and in equidistant lines, and the terrain is flat (except, if otherwise mentioned). We also assume that the covered area consists of n overlapping parallel strips of equal length, and the flying speed and the flying height over ground are constant.

For most of the relations, numerical examples are given. In these examples, the following typical input values are used.

$\Delta t = 0.1$ ns; $v = 216$ km/h ($= 60$ m/s); $\theta = 30$ deg; $\gamma = 1$ mrad ($= 0.0573$ deg); $F = 10$ kHz; $f_{sc} = 30$ Hz; $h = 750$ m; $T_f = 3$ h ($= 10{,}800$ s); $W = 10$ km; $L = 15$ km; $q = 15\%$; $t_{min} = t_p = 10$ ns; $t_{rise} = 1$ ns.

2. Relations and formulas for laser ranging

2.1. Range and range resolution

Pulse laser:

$$R = c\frac{t}{2}; \quad \Delta R = c\frac{\Delta t}{2}$$

The time t is measured by a time interval counter relative to a specific point on the pulse, e.g., the leading edge (rising side of the pulse). Since the leading edge is not well-defined (no rectangular pulses), the time is measured for a point on the leading edge, where the signal voltage has reached a predetermined threshold value. This is accomplished with a threshold trigger circuit to start and stop the time counting. A possible error occurs if the voltage magnitudes of the transmitted and received pulses are not adjusted to the same value before they are sent to the time interval counter, i.e., if the received pulse amplitude is too low, the measured time t will be too long, and the opposite. This signal adjustment takes place at the amplifier before the threshold detection circuits. To reduce the time jitter (''time walk'') caused by varying pulse amplitudes, instead of constant threshold discriminators, constant fraction ones are generally used, which define the time point as a constant fraction of the signal peak.

CW laser:

$$R = \frac{1}{4\pi}\frac{c}{f}\varphi; \quad \Delta R = \frac{1}{4\pi}\frac{c}{f}\Delta\varphi$$

Example: CW laser: $f_{high} = 10$ MHz, phase resolution $\Delta\phi/2\pi = 1/16384$ (14-bit quantisation): $\Delta R = 0.9$ mm. To get the same range resolution with a pulse laser, Δt should be 6.1 ps.

For ALS, the resolution is usually of lesser importance (since in most cases it is much lower than the accuracy), as long as it is sufficiently small that the highest range accuracy can be achieved and small enough to permit accuracy investigations through repeated measurements, etc.

2.2. Maximum unambiguous range

For pulse lasers, the maximum unambiguous range depends on various factors: (1) the maximum range (number of bits) of the time interval counter, and (2) the pulse rate. To avoid confusion in the pulses arriving at the time interval counter, it is usually a requirement that no pulse is transmitted until the echo of the previous pulse has been received. For example, for a pulse rate of 25 kHz, the maximum unambiguous range is 6 km.

In practise, the above factors almost never limit the maximum range (and flying height). This is rather limited by other factors like laser power and beam divergence, atmospheric transmission, target reflectivity, detector sensitivity, increasing influence of flying height and attitude errors on the 3D positional accuracy, etc.

For CW laser:

$$R_{max} = \frac{\lambda_{long}}{2}$$

Example: A CW laser employs two frequencies of 1 MHz and 10 MHz. The low frequency corresponds to a wavelength of 300 m, i.e., 150 m unambiguous range. This does not imply that the flying height over ground must be limited to 150 m. Latter can be increased by: (a) complementary height information from other navigation sensors, given that they provide height with an accuracy < 150 m; (b) range gating, i.e., when the range of possible distances to the object is known a priori to be less than 150 m;

and (c) starting the measurements from a range < 150 m and continuous tracking of the range, given that no range discontinuities of > 150 m occur between consecutive measurement points.

Keeping all other conditions constant, maximum range is typically proportional to the square root of reflectivity, and to the square root of the laser power. Best range performance is achieved when the atmosphere is cool, dry and clear. IR energy propagation (and range) is severely attenuated by water vapour (in the forms of rain, fog, and/or humidity) and carbon dioxide in the atmosphere (to avoid this, ALS systems select IR wavelengths with high atmospheric transmission). Dust particles and smoke also reduce detection range. Regarding time of day, the best results are achieved during night, and the worst during day with bright sunlight.

2.3. Ranging precision

$$\sigma_{\mathrm{R}} \sim \frac{1}{\sqrt{\mathrm{S/N}}}$$

Pulse laser: $\sigma_{\mathrm{R}_{\mathrm{pulse}}} \sim \frac{c}{2} t_{\mathrm{rise}} \frac{\sqrt{B_{\mathrm{pulse}}}}{P_{\mathrm{R}_{\mathrm{peak}}}}$

CW laser: $\sigma_{\mathrm{R}_{\mathrm{cw}}} \sim \frac{\lambda_{\mathrm{short}}}{4\pi} \frac{\sqrt{B_{\mathrm{cw}}}}{P_{\mathrm{R}_{\mathrm{av}}}}$,

with $P_{\mathrm{R}_{\mathrm{peak}}}$ the received peak optical power and $P_{\mathrm{R}_{\mathrm{av}}}$ the received average optical power.

For CW lasers, the ranging precision is proportional to the square root of the signal bandwidth (measurement rate), since the latter is inversely proportional to the number of cycles averaged to get one measurement.

Gardner (1992) gives the following relation for the range variance for satellite laser altimeters, which however can be used with some modifications for ALS, too. Note that the last term of the equation below, unlike the proportionalities above, takes into account also the error of the pointing angle (for scanners, the instantaneous scan angle).

$$\sigma_{\mathrm{R}}^2 = \left(\frac{F}{\mathrm{PE}}\right)\sigma_{\mathrm{w}}^2 + \left(\frac{4}{9}\right)\left(\frac{\sigma_{\mathrm{w}}}{\Delta t}\right)\left(\frac{\sigma_w^2}{2^{2\mathrm{NB}}}\right) + \left(\frac{\Delta t^2}{12}\right) + \left[h\frac{\tan(\theta+i)\,\sigma_\theta}{\cos(\theta+i)}\right]^2,$$

with F = detector (excess) noise factor; PE = number of signal photoelectrons in the receiver pulse; σ_{w} = rms received pulse width (function of surface incident angle, beam curvature, surface roughness, transmitted laser pulse width, and receiver impulse response); NB = number of amplitude bits in digitiser sampling; h = height over ground; θ = pointing angle with respect to nadir; i = surface slope; $\theta + i$ = incidence angle; σ_θ = rms pointing error.

2.4. Laser power and energy

$$E = P_{\mathrm{peak}}\, t_{\mathrm{p}},$$

i.e., for a given energy, the shorter the pulse duration, the higher the pulse power, both sent and received, and the smaller the pulse detection error.

$$P_{\mathrm{av}} = EF;\ P_{\mathrm{av}} = P_{\mathrm{peak}}\, t_{\mathrm{p}} F$$

For a given average power, the higher the pulse rate, the lower the pulse energy. The latter means that for a given pulse duration, the peak power should also decrease, if the pulse rate increases.

Example: $P_{\mathrm{peak}} = 2$ kW, $t_{\mathrm{p}} = 10$ ns, $F = 10$ kHz: $P_{\mathrm{av}} = 0.2$ W.

2.5. Relation between transmitted and received power (range equation)

Assumptions:

Diffuse circular target. The laser footprint completely covers the entire target area that reflects the beam back to the source. The reflected power radiates uniformly into a hemisphere.

Illuminated area:

$$A_{\mathrm{I}} = \frac{\pi}{4}(D + R\gamma)^2,$$

with γ in radian.

Power density within above area (assumed to be uniform):

$$\Phi_{\mathrm{tar}} = \frac{P_{\mathrm{T}}}{A_{\mathrm{I}}} M$$

Total power reflected from the target:

$$P_{\text{refl}} = \frac{\rho}{\pi} \Phi_{\text{tar}} A_{\text{tar}},$$

with

$$A_{\text{tar}} = \frac{\pi D_{\text{tar}}^2}{4}$$

and ρ/π an assumed Lambertian BRDF. The power reflected from the target, that is collected by the receiver optics, with M the atmospheric transmission and A_r the receiver area, is:

Power collected by the receiver:

$$P_r = P_{\text{refl}} \quad M \frac{A_r}{R^2},$$

with

$$A_r = \frac{\pi D_r^2}{4}$$

Combining the above equations yields:

$$P_r = \rho \frac{M^2 D_r^2 D_{\text{tar}}^2}{4R^2 (R\gamma + D)^2} P_T$$

For large R, D can be neglected in comparison to $R\gamma$ and the above equation reduces to:

$$P_r = \rho \frac{M^2 D_r^2 D_{\text{tar}}^2}{4R^4 \gamma^2} P_T$$

Assuming $A_I = A_{\text{tar}}$, the above equation becomes

$$P_r = \rho \frac{M^2 A_r}{\pi R^2} P_T$$

The above equation can also be used with the transmitted and received energy per pulse instead of the power. It is a rather optimistic approximation, since there are additional losses, e.g., due to the optical transmission of the transmitter and receiver optics, and the narrow bandpass filter at the receiver to exclude background radiation. The equation makes clear that, in order to get useful signal with high flying heights, the transmitted power and the receiver optics dimensions should be increased and the beam divergence decreased.

Example (pulse laser, 1064 nm wavelength):

$P_T = 2$ kW, $\gamma = 10^{-3}$ rad, $R = 750$ m, $D_{\text{tar}} = 70$ cm, $D_r = 10$ cm, $M = 0.8$, $\rho = 0.5$

$P_r = 1.2 \times 10^{-9} P_T = 2.4 \times 10^{-6}$ W

Assuming a peak power of 2 KW and a pulse width of 10 ns, the transmitted pulse energy would be 20 μJ, and the received one just 24 fJ!

If we assume that the optical transmission of the transmitting and receiving optics and of the bandpass filter are 0.8, the above values of received power and energy would be further reduced by 50%. It is clear that the received power strongly depends on the range (inversely proportional to the 2nd power of range) and is a very small fraction of the transmitted power. It is also obvious that if a very small fraction of the transmitted signal comes back to the optics, then this could be falsely detected as a target echo. This can be avoided by close-range suppression techniques and other means.

The number of received photoelectrons per pulse will be

$$N_r = \eta \frac{E_r}{H\nu},$$

with η the detector quantum efficiency, H the Planck constant $= 6.626 \times 10^{-34}$ J s, ν the laser frequency, and $H\nu$ the energy per photon.

Assuming a Nd:YAG laser with 1064 nm wavelength, a detector quantum efficiency of 0.3, and received power of 24 fJ, then $H\nu = 1.87 \times 10^{-19}$ J and $N_r = 38{,}500$ photoelectrons.

The S/N can be estimated according to the simplified relation (ignores some other possible noise sources, like thermal noise)

$$\text{S/N} = \frac{N_r}{\sqrt{F(N_r + N_B) + N_D}},$$

with N_r the signal photoelectrons, N_D the dark noise photoelectrons, N_B the background photoelectrons, F the excess noise factor of detector.

Assuming $N_r = 385$ (i.e., 100 times less than the example above, for a weak ground return), $F = 3$, $N_D = 10$, $N_B = 100$, then $\text{S/N} = 10 \mathrel{\hat{=}} 20$ dB.

2.6. Vertical resolution (minimum separation between objects along the pulse path)

$$R_{\min} = c\frac{t_{\min}}{2}$$

Example: $t_{\min} = 10$ ns: $R_{\min} = 1.5$ m.

2.7. Minimum detectable object

The minimum detectable object within the laser footprint does not depend on the object's size, but primarily on its reflectivity. Let's assume that the sensor is capable of measuring the distance to a flat and even surface (area A) with a reflectivity of just 5%. Then, the minimum area of a detectable object (reflectivity 100%) at the same distance would become $A/20$. For example, with a laser footprint of 0.5 m, the illuminated area is 0.2 m^2 and the minimum size of a detectable object would be 0.01 m^2 (10 cm × 10 cm or 2 cm × 50 cm, etc.). Note that in the above considerations, several factors that influence detectability like range, laser power, atmospheric conditions, background irradiation, type of target reflectivity (diffuse, specular, diffuse and specular), terrain inclination, target 3D structure, laser aperture, detector sensitivity and noise level, laser wavelength, etc., have been ignored.

Examples: Branch of an apple tree 3 cm diameter nondetectable; twisted aluminium cable 1 cm diameter detectable; grain and dust of pit coal nondetectable; crumbs of pit coal detectable (behave like corner reflectors).

3. Relations and formulas for airborne laser scanning

3.1. Minimum laser beam divergence (diffraction limited)

$$\mathrm{IFOV}_{\mathrm{diff}} = 2.44\frac{\lambda}{D}$$

Example: $\lambda = 1064$ nm, $D = 10$ cm: $\mathrm{IFOV}_{\mathrm{diff}} = 0.026$ mrad.

3.2. Laser footprint diameter

$A_L = D + 2h \tan(\gamma/2)$ (see Fig. 1a)
and since D is generally small (ca. 10–15 cm),
$A_L = 2h \tan(\gamma/2)$ (see Fig. 1b)
and since γ is small,

$$A_L = h\gamma,$$

with γ in radian,i.e., for every 100 m of flying height, the laser footprint is 1/10th of the laser beam divergence (in milliradian).

Example: $h = 750$ m; $\gamma = 1$ mrad: $A_L = 0.75$ m.

3.2.1. Generalisation of second equation in Section 3.2. for inclined terrain (see Fig. 1c)

$$A_L = \frac{a * 2h \sin\left(\frac{\gamma}{2}\right)}{\cos\left(\theta_{\mathrm{inst}} - \frac{\gamma}{2}\right)}$$

with $a = [\cos e + \sin e \tan(e + \gamma/2)]$ and $e = \theta_{\mathrm{inst}} + i$; i = inclination angle of local planar terrain surface, plane inclined in across track direction, $i > 0$ for negative inclination, i.e., plane moves away from the laser beam, else negative; A_L becomes infinity, if $i = 90 - \theta_{\mathrm{inst}} - \gamma/2$.

Example:
$i = 0$, $\theta_{\mathrm{inst}} = 0$: $A_L = 0.75$ m
$i = 0$, $\theta_{\mathrm{inst}} = 15$ deg: $A_L = 0.80$ m
$i = 45$ deg, $\theta_{\mathrm{inst}} = 0$: $A_L = 1.06$ m (in across track direction, while along track, the footprint diameter remains 0.75 m).

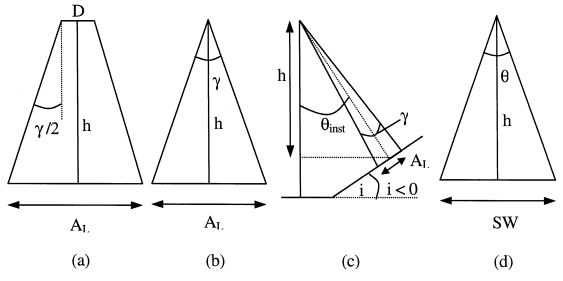

Fig. 1. (a,b,c) Used for the definition of the laser footprint, (d) for the swath width.

3.2.2. Generalisation of second equation in Section 3.2. for flat terrain and variable instantaneous scan angle

$$A_{L_{inst}} = h\left[\tan\left(\theta_{inst} + \frac{\gamma}{2}\right) - \tan\left(\theta_{inst} - \frac{\gamma}{2}\right)\right]$$

or

$$A_{L_{inst}} = \frac{h}{\cos^2(\theta_{inst})}\gamma,$$

with γ in radian.

Example: $h = 750$ m, $\theta_{inst} = 15$ deg, $\gamma = 1$ mrad: $A_L = 0.80$ m.

3.3. Minimum flying height over ground

This can be limited due to platform specifications, state regulations (often different for urban and other areas), and eye safety range.

3.4. Swath width (see Fig. 1d)

$$SW = 2h\tan\left(\frac{\theta}{2}\right) = ah,$$

with $a = 2\tan(\theta/2)$.

The above formula is valid also for an elliptical scan, for $\theta/2$ being the angle measured from the nadir direction perpendicular to the flight direction. For a *Z*-shaped scan, the actual scan line length between left and right swath border is a bit larger than the swath width (see Fig. 2), but the difference is very small.

Example: $h = 750$ m; $\theta = 30$ deg: SW = 402 m, $a = 0.54$.

3.5. Number of points per scan line

$$N = F/f_{sc}$$

Note that N is independent of flying height over ground and swath width.

Example: $F = 10$ kHz, $f_{sc} = 30$ Hz: $N = 333$.

3.6. Along track point spacing

$$\mathrm{d}x_{along} = v/f_{sc}$$

(note that $\mathrm{d}x_{along}$ is independent of the flying height, contrary to the average $\mathrm{d}x_{across}$ below).

Example: $v = 60$ m/s; $f_{sc} = 30$ Hz: $\mathrm{d}x_{along} = 2$ m.

For an elliptical scan, the above formula gives the largest point distance between two neighbouring scan lines, i.e., the distance for points in the middle of the swath width (nadir). For a *Z*-shaped scan, it gives the distance along track between corresponding points

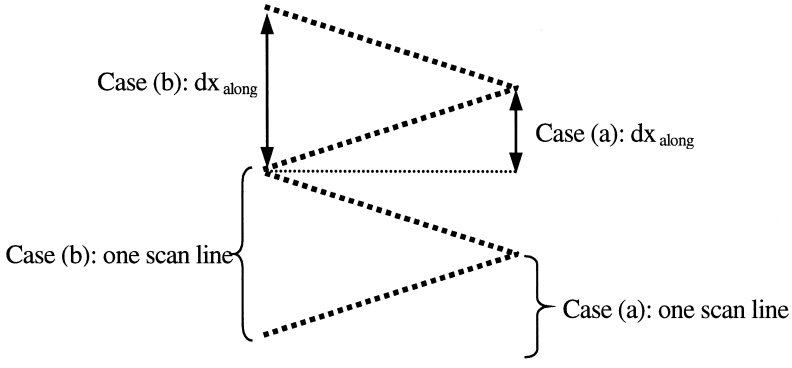

Fig. 2. Two possible scan line definitions with *Z*-shaped scan.

of two consecutive scan lines, e.g., 3rd point of scan line i to 3rd point of scan line $i+1$. Since there can be two definitions of a scan line with Z-shaped scans, the along-track spacing can vary (see Fig. 2).

3.7. Across track point spacing

Assuming equal distance between points along scan line and flat terrain:

$$\mathrm{d}x_{\mathrm{across}} = \mathrm{SW}/N.$$

Example: SW = 402 m, $N = 333$: $\mathrm{d}x_{\mathrm{across}} = 1.21$ m.

For a Z-shaped scan (see Fig. 2), two cases are distinguished: (a) a scan line is defined as a scan from left to right swath border or the opposite, (b) a scan line is defined as a full bidirectional scan from left to right and right to left or the opposite. In case (a), the above formula is approximately correct. In case (b), $\mathrm{d}x_{\mathrm{across}}$ should be multiplied by 2, since the number of points N are distributed over approximately twice the swath width.

For a fiber scanner:

$$\mathrm{d}x_{\mathrm{across}} = h\frac{\theta}{N-1}$$

For an elliptical (nearly circular) scan, across-track spacing is approximately given by

$$\mathrm{d}x_{\mathrm{across}} = \pi\ \mathrm{SW}/N$$

and a more accurate formulation for an inclination angle of the rotation axis AN = 45 deg (see Fig. 9 left, in Wehr and Lohr, 1999) is given by

$$\mathrm{d}x_{\mathrm{across}} = \frac{4.4429h}{N}\sqrt{\tan^2(2\mathrm{SN}) + \tan^2(1.41\mathrm{SN})},$$

with SN = inclination angle of mirror with respect to the plane, normal to the rotation axis (see Fig. 9 left, in Wehr and Lohr, 1999).

Assuming even distribution of points along the scan line with respect to the scan angle (constant scan speed), i.e., not equidistant on the ground, and flat terrain:

$$\mathrm{d}x_{\mathrm{across}_{\mathrm{inst}}} = h(\tan\theta_2 - \tan\theta_1),$$

with 1,2 consecutive points, point 1 closer to nadir, θ_1 and θ_2 instantaneous scan angles, and $\theta_2 - \theta_1 = \Delta\theta = \theta/(N-1)$ = angle step or

$$\mathrm{d}x_{\mathrm{across}_{\mathrm{inst}}} = \frac{h}{\cos^2(\theta_{\mathrm{inst}})}\frac{\dot{\theta}_{\mathrm{inst}}}{F},$$

with $\dot{\theta}_{\mathrm{inst}}$ the instantaneous angular speed in radian per second.

Example: $\theta = 30$ deg; $N = 333$, $\Delta\theta = 0.09$ deg, $h = 750$ m: $\mathrm{d}x_{\mathrm{across}_{\mathrm{inst}}}$ (nadir) = 1.18 m; $\mathrm{d}x_{\mathrm{across}_{\mathrm{inst}}}$ (swath border) = 1.26 m.

For same assumptions as above, whereby $h_2 = h_1$ and $\Delta = h - h_1$, i.e., if $\Delta h > 0$, flat terrain lies above average flying height over terrain h:

$$\mathrm{d}x_{\mathrm{across}} = (h - \Delta h)(\tan\theta_2 - \tan\theta_1)$$
$$= h_1(\tan\theta_2 - \tan\theta_1)$$

Example: $\Delta h = +150$ m/−150 m: $\mathrm{d}x_{\mathrm{across}}$ (at nadir) = 0.94 m/1.41 m; $\mathrm{d}x_{\mathrm{across}}$ (at swath border) = 1.01 m/1.51 m.

For same assumptions as above, but assuming that laser points 1 and 2 lie on a plane with inclination angle i with respect to horizontal (inclination angle in across track direction):

$$\mathrm{d}x_{\mathrm{across}} = h_1(\tan\theta_2 - \tan\theta_1)(1 + a),$$

with $a = \sin\theta_2 \cos\theta_2 [\tan(\theta_2 + i) - \tan\theta_2]$ and $i > 0$ for negative inclination, i.e., plane inclined away from the laser beam direction, else negative.

Example: $h_1 = h = 750$ m, $\theta_1 = 0/\theta_2 = 0.09$ deg (nadir), $\theta_1 = 14.91$ deg/$\theta_2 = 15$ deg (swath border), $i = 45$ deg: $\mathrm{d}x_{\mathrm{across}} = 1.18$ m (nadir), $\mathrm{d}x_{\mathrm{across}} = 1.72$ m (swath border).

3.8. Required number of strips

$n = \min(n_i)$ such that $(n_i - 1) \geq (W - \mathrm{SW})/[\mathrm{SW}(1 - q/100)]$.

For corridor mapping, usually $n = 1$.

Example: $W = 10$ km, $q = 15\%$, SW = 402 m: $n = 30$.

In practice, during flight planning, the flying height is selected according to the lowest point to be measured, while the strip overlap is calculated based on the highest points to avoid gaps caused by narrow swaths.

3.9. Area covered

$$A = \mathrm{SW}\, v T_s \left[(n-1)\left(1 - \frac{q}{100}\right) + 1 \right]$$
$$= \mathrm{SW}\, L \left[(n-1)\left(1 - \frac{q}{100}\right) + 1 \right],$$

with $T_s = L/v$.

For $n = 1$ (e.g., in corridor mapping): $A = \mathrm{SW}\ vT_s = \mathrm{SW}\ L$.

Example: $L = 15$ km, $v = 60$ m/s, $q = 15\%$, SW $= 402$ m, $n = 30$: $T_s = 250$ s, $A = 154.7$ km^2.

3.10. Point density per unit area

$$d = FnT_s/A$$

Example: $A = 154.7$ km^2, $T_s = 250$ s, $n = 30$, $F = 10$ kHz: $d = 0.485$ points/m^2.

3.11. Oversampling / undersampling, i.e., relation of laser footprint to point spacing

$Q_{\mathrm{across}} = 100\ A_L / \mathrm{d}\, x_{\mathrm{across}}$; if $Q_{\mathrm{across}} > 100\%$, then oversampling, else undersampling.

Assuming quadratic laser footprint. Similar formula for oversampling/undersampling factor in flying direction Q_{along}. Strictly speaking, the above formula should be evaluated for the instantaneous laser footprint and across- and along-track spacing.

Example: $A_L = 0.75$ m, $\mathrm{d}\, x_{\mathrm{across}} = 1.18$ m, $\mathrm{d}\, x_{\mathrm{along}} = 2$ m: $Q_{\mathrm{across}} = 63.6\%$ undersampling, $Q_{\mathrm{along}} = 37.5\%$ undersampling.

3.12. Data amount

Data amount refers to the 'final' data (but no interpolated regular grid), not the data generated during laser scanning. Assuming 21 bytes per measurement point to record point number, X, Y, Z, time and quality code, binary storage, 4 bytes for each of the five first data and 1 byte for quality code (point number could be skipped). For intensity recording, 1 byte per point should be added and for multiple echoes per pulse, multiply the total with the number of echoes per pulse.

$$C = FT_f * 21 \text{ bytes}$$

Example: $F = 10$ kHz, $T_f = 3$ h: $C = 2.268$ GBytes or 0.756 GBytes/h.

3.13. Travel distance of the aircraft between sending and receiving pulse

$$s = 2vR/c$$

Example: $v = 60$ m/s, $R = 750$ m: $s = 0.3$ mm!

3.14. Deflection by an oscillating mirror

Oscillating mirrors can have one or two axes, and can scan uni- or bidirectionally. A mirror with bidirectional scan creates a Z-shaped pattern, which is quite common and described below. A mirror with unidirectional scan creates parallel lines or curves. Bidirectional mirrors with two axes can create a meanderwise parallel line pattern on the ground, while the scan pattern itself is like an ∞.

A complete scan ranges from $-\theta/2$ to $+\theta/2$. At each end, the oscillating mirror has to change scan direction and thus should have zero speed. In general, there are a number of theoretical solutions out of which two are explained below.

3.14.1. Constant angular speed

Left to right:

$$\theta_{\mathrm{inst}} = -\frac{\theta}{2} + \dot{\theta} t,$$

with t the scan time measured from the swath border;

$$\dot{\theta} = \mathrm{const} = \frac{\theta}{f_{sc}}$$

Right to left:

$$\theta_{\mathrm{inst}} = \frac{\theta}{2} + \dot{\theta} t; \quad \dot{\theta} = -\mathrm{const}.$$

During motion:

$\ddot{\theta} = 0$; at turn $\ddot{\theta} = \pm\infty$

It is obvious that using a *Z*-shaped scan and applying constant speed will require extreme high accelerations and decelerations at the turn. An alternative can be to use a constant speed over almost the whole swath width and at the swath borders increase/decrease the angular speed from 0 to the constant speed or the opposite.

3.14.2. Sinusoidal angular speed

$$\dot{\theta} = -\frac{\theta}{2}\,\omega \sin \omega t; \quad \ddot{\theta} = -\frac{\theta}{2}\,\omega^2 \cos \omega t,$$

with $\omega = 2\pi f_{sc}$, where f_{sc} is the scan rate for a complete right to left and left to right scan.

With a sinusoidal motion, the mechanical requirements are less stringent and thus provide a better stability and reliability of the mirror mechanics. But assuming a constant flight speed, the scan pattern on the ground also becomes a sinusoidal curve. Points along the scan are not equidistant.

3.15. Rotating mirrors or prisms

Rotating mirror scanners have a constant angular speed, so the above formulas for oscillating mirrors can be applied to them. Since the scan in this case is unidirectional, there is no turn in the scan. Given a rotation mirror with k facets and a rotation speed of ν rotations per second (rps), the scan rate f_{sc} is given by

$f_{sc} = k\nu$.

Each mirror facet occupies a sector u of the scan mirror: $u = 360/k$ (in degree); and the theoretical scan angle of each line (in degree) is: $\theta_t = 2u = 720/k$.

To avoid laser pulses that reflect from the two borders of each mirror sector, either the receiver is blanked during this period, or the receiving telescope FOV is set smaller than the scan angle in order to truncate the border laser pulses. Thus, the effective scan angle θ is decreased by the truncation factor t_f (< 1). The effective pulse rate and the effective number of points per scan line are also decreased by the truncation factor. The angular step is not changed by the truncation and is given in degree by

$\Delta\nu = 720\nu/F$,

with F the laser pulse rate (not the effective one).

4. Accuracy of 3D positioning

The accuracy of 3D coordinates depends on many factors. The main factors are the accuracy of (a) range, (b) position of the laser beam, and (c) direction of the laser beam. Since the results are usually in WGS84, the final results also depend on the accuracy of the transformation from WGS84 to the local coordinate system, including corrections for the geoid undulations, which can be significant with respect to the accuracy potential of ALS. In addition, since range, position, and beam direction are measured by different sensors, any time misregistration errors will also influence the results.

4.1. Some major accuracy factors

4.1.1. Range accuracy

The range accuracy is the most complicated among the major accuracy factors. In practice, however, if the necessary measures and precautions are taken, the contribution of range errors to 3D coordinate errors is the minimum among the major error sources, with the exception of low flying heights and small scan angles, where its relative importance with respect to the total error budget increases.

The range accuracy of pulse lasers is mainly dependent on the following factors:

- Ability to select the same relative position on the transmitted and received pulse in order to measure the time interval. This is limited by noise, signal strength and sensitivity of the threshold detector, and shortness and reproducibility of the transmitter pulse. The main factor here is the steepness of the received signal, i.e., the rise time of the pulse. A typical laser pulse with a duration of 10 ns has a rise time of approximately 1 ns (1 ns corresponds to 30 cm distance or 15 cm range). Rise time is independent of the pulse width. For a detector, the rise time depends

on the incident light wavelength and the load resistance. However, although small rise time requires low load resistance, high sensitivity requires the opposite. Thus, the steepness of the pulse can be increased by increasing the receiver bandwidth, but this also leads to a decrease of the S/N.

- The accuracy with which fixed time delays in the system are known, e.g., counter (frequency) instability can lead to drift systematic errors.
- The accuracy of the time interval counter, e.g., resolution, time jitter (bit jitter, random error). The time counter has a resolution of ca. 0.1 ns (typical values 0.05–0.2 ns), which would correspond to a range resolution of 1.5 cm.

Example of rise time and range accuracy:Let's assume a corn field of 1 m height and a 10-ns pulse. Part of the laser light will be reflected at the top of the plants and another part from the leaves beneath and the ground. Thus, the complete echo will become a mixture of a lot of echoes from very small surfaces. For simplicity, it is assumed that all reflecting surfaces are evenly distributed over the 1-m height. The rise time of the echo will become 7.6 ns (i.e., rise time of transmitted pulse (1 ns) and extension caused by surface roughness, i.e., 6.6 ns corresponding to 2×1 m height). Therefore, the measured distance will be anywhere between top and bottom of the plants. In case of flat, rigid terrain (e.g., streets), the pulse detection accuracy should be 10–15% of the rise time, e.g., for 1 ns rise time, this would correspond to 1.5–2.25 cm range accuracy.

The range accuracy of CW lasers mainly depends on the following:

- Frequency of the tone or modulation
- Accuracy of the phase measurement loop. This depends on signal strength, noise, etc.
- Stability of the modulation oscillator
- Number of cycles (measurements) that can be averaged together for a range measurement
- Turbulence and variations in the index of refraction

For low pulse rates, the main limiting factor is long-term drift and fluctuations due to small signal variations, for higher pulse rates, the detector thermal noise, and for the highest pulse rates, the resolution of the timer.

For both pulse and CW lasers, effects from the optical elements (mirrors, optical windows) can influence range accuracy. Such effects include the following:

- Reflection of light to the sensor, e.g., solar background irradiation (can be reduced by a narrow bandpass filter), reflection of a portion of the outgoing laser beam back into the sensor (optical cross-talk)
- Attenuation of light passing through a window or reflecting off a mirror
- Scattering of light by a window or mirror (caused also by dust and/or imperfections on the surface or in the body of the optical element)
- Slowing of light passing through a window
- Curved windows (can cause defocusing of transmitted and received beam)

As far as the detector is concerned, the following properties are desired:

- A large response at the wavelength to be detected
- A small value for the additional noise introduced by the detector
- Sufficient speed of response (i.e., small rise time)

The main noise sources in detectors, apart from the shot noise (of the signal and the dark current), are thermal (called sometimes Johnson) noise, which is proportional to the square root of the sample (measurement) rate, and $1/f$ noise (called also excess noise, since it exceeds shot noise at low frequencies).

In addition to noise, there are other factors that affect range. The most significant ones, are the amplitude of the received signal (which also depends on target reflectivity and local surface normal), and mixed echoes due to vertical target structure (e.g., with vegetation, rough or discontinuous terrain and large laser footprint) or multiple targets within the laser footprint (e.g., small strong reflecting targets at the border of the laser footprint) or averaging of cycles over discontinuous surfaces with CW lasers. Temperature and ambient light level can also affect the accuracy slightly, but these effects are generally compensated. If the necessary precautions are taken, the ranging accuracy has a small dependence on the distance to the target.

4.1.2. Position accuracy

This depends mainly on the quality of the DGPS postprocessing. Other factors: GPS hardware, GPS satellite constellation during flight, number, distribution and distance of ground reference stations from aircraft (values of 10–100 km have been reported), accuracy of offsets and misalignment between GPS and INS, and INS and laser scanner (depending on the used computation method less information might be sufficient, e.g., offset between GPS and laser and misalignment between INS and GPS, or offset and misalignment between laser and INS), and the accuracy of the laser beam direction (scanner accuracy). The GPS error varies over time, but it is bounded (exceptions can occur during GPS outage), and through integration of GPS with INS, the temporal variability is smoothed. Typically, with DGPS and postprocessing, accuracies of 5–15 cm can be achieved.

4.1.3. Attitude accuracy

This depends on the quality of the INS, the INS frequency (i.e., interpolation error), the method of postprocessing and integration with the GPS. Heading accuracy in addition depends on latitude. The effect of attitude errors on the 3D accuracy increases with the flying height and the scan angle.

4.1.4. Time offsets

For accurate 3D positioning, orientation, position, and range are required to be taken at the same time. If there is a time offset and this is not known precisely, it will cause a variable error. The error increases with increasing change rate of the related measurements, e.g., while a time offset between range and rotation angles can have a small effect for a calm flight (rotation angles remain fairly stable), it can influence the 3D accuracy a lot for a turbulent flight.

Concluding, the total error consists of a variable part that is dependent on major parameters like flying height, scan angle, terrain topography, and land cover (referring to object geometry and reflectivity) and a constant part (5–10 cm in good cases) that is independent of the previous parameters, e.g., pulse detection accuracy, GPS accuracy, etc.

4.2. Influence of various error sources on accuracy of 3D coordinates

In the following, we will ignore different possible error sources, like time offsets, insufficient calibration of offset and misalignment between the various sensors, possible errors in the transformation in the local coordinate system, number, distribution and distance of GPS reference stations, quality of GPS/INS postprocessing, correction of relative errors through block adjustment of the strips, etc.

Let us assume, that the terrain is flat and scanning is performed in a vertical plane perpendicular to the flight direction. Latter assumption is quite valid, except for the elliptical Palmer scan. It is also assumed that the angles ω (ω the rotation around the flight direction) and ψ (ψ the rotation around the across-track direction) are both zero, i.e., horizontal flight (see Fig. 3). The rotation angle κ (κ the rotation around the vertical axis) can have any value. We define a local right-handed system x, y, z centred at the laser beam origin (centre of scan mirror) and a right-handed object coordinate system X, Y, Z with origin the nadir of the origin of the local coordinate system. The positive x-axis is in the flight direction. The attitude errors $\Delta\omega$, $\Delta\psi$, $\Delta\kappa$ refer to rotation errors around the respective axes of the local coordinate system. κ is the rotation from the X axis to the x axis. β is the scan angle,

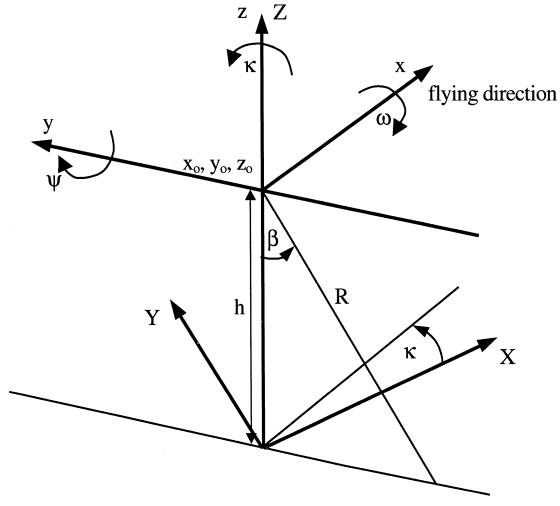

Fig. 3. Coordinate systems used and rotation angles.

Table 1
Effect of different error sources on accuracy of X, Y, Z coordinate errors (in centimeter)

Coordinate error	Flying height (m)	Scan angle β (deg)	Error due to $\Delta\omega$	Error due to $\Delta\psi$	Error due to $\Delta\kappa$	Error due to $\Delta\beta$	Error due to ΔR	Error due to Δx_0	Error due to Δy_0	Error due to Δz_0	Total error
ΔX		0			0/0		0/0				22.4/24.5
		−7.5			3.7/2.6		0/−0.5				22.7/24.7
	400	−15	0/14.8	20.9/14.8	7.5/5.3	0/9.9	0/−0.9				23.6/25.1
		−30			16.1/11.4		0/−1.8				27.6/27.1
		0			0/0		0/0	8/5.7	0/−5.7	0	53.0/58.4
		−7.5			9.2/6.5		0/−0.5				53.8/58.8
	1000	−15	0/37.0	52.4/37.0	18.7/13.2	0/24.7	0/−0.9				56.2/59.9
		−30			40.3/28.5		0/−1.8				66.6/65.0
ΔY		0			0/0		0/0				26.4/24.5
		−7.5			0/2.6		0.7/0.5				26.4/24.7
	400	−15	−20.9/−14.8	0/14.8	0/5.3	−14/−9.9	1.3/0.9				26.4/25.1
		−30			0/11.4		2.5/1.8				26.5/27.1
		0			0/0		0/0	0/5.7	8/5.7	0	63.5/58.4
		−7.5			0/6.5		0.7/0.5				63.5/58.8
	1000	−15	−52.4/−37.0	0/37.0	0/13.2	−35/−24.7	1.3/0.9				63.5/59.9
		−30			0/28.5		2.5/1.8				63.6/65.0
ΔZ		0	0			0	5				9.4
		−7.5	2.8			2	5				10.0
	400	−15	5.6			4	5				11.7
		−30	12.1			8	4				17.0
		0	0	0 (very small)	0	0	5	0	0	8	9.4
		−7.5	6.9			5	5				12.7
	1000	−15	14			9	5				19.1
		−30	30.2			20	4				37.3

Values given for $\kappa = 0$ deg/45 deg.

$\beta \in [\theta/2, -\theta/2]$, i.e., it has positive values for scans to the left of the flying direction, else negative.

4.2.1. Influence of $\Delta\omega$

With $\Delta x = 0$; $\Delta y = h\ [\sin(\beta + \Delta\omega) - \sin(\beta)]/\cos(\beta) = h \sin(\Delta\omega) \approx h\ \Delta\omega$, with $\Delta\omega$ in radian.

Influence on X and Y is: $\Delta X = -\Delta y \sin(\kappa) \approx -h\ \Delta\omega \sin(\kappa)$; $\Delta Y = \Delta y \cos(\kappa) \approx h\ \Delta\omega \cos(\kappa)$.

Influence on Z is: $\Delta Z = h\ [1 - \cos(\beta + \Delta\omega)/\cos(\beta)] \approx h\ \Delta\omega \tan(\beta)$, with $\Delta\omega$ in radian.

4.2.2. Influence of $\Delta\psi$

With $\Delta x = -h \sin(\Delta\psi)$; $\Delta y = 0$.

Influence on X and Y is: $\Delta X = \Delta x \cos(\kappa) = -h \sin(\Delta\psi) \cos(\kappa)$; $\Delta Y = \Delta x \sin(\kappa) = -h \sin(\Delta\psi) \sin(\kappa)$.

Influence on Z is: $\Delta Z = h\ [1 - \cos\ \Delta\psi]$.

4.2.3. Influence of $\Delta\kappa$

Influence on X and Y is:
$\Delta X = -h \tan(\beta)\ [\sin(\kappa + \Delta\kappa) - \sin(\kappa)]$ and for $\kappa = 0$ deg, $\Delta X = -h \tan(\beta)\ [\sin(\Delta\kappa)]$;
$\Delta Y = h \tan(\beta)\ [\cos(\kappa + \Delta\kappa) - \cos(\kappa)]$ and for $\kappa = 0$ deg, $\Delta Y = h \tan(\beta)\ [\cos(\Delta\kappa) - 1] \approx 0$ for small $\Delta\kappa$.

Influence on Z is zero.

4.2.4. Influence of scan mirror angle errors $\Delta\beta$

It is similar to the $\Delta\omega$ errors, i.e., with $\Delta x = 0$; $\Delta y = h\ [\sin(\beta + \Delta\beta) - \sin(\beta)]/\cos(\beta) = h \sin(\Delta\beta) \approx h\ \Delta\beta$, with $\Delta\beta$ in radian.

Influence on X and Y is: $\Delta X = -\Delta y \sin(\kappa) \approx -h\ \Delta\beta \sin(\kappa)$; $\Delta Y = \Delta y \cos(\kappa) \approx h\ \Delta\beta \cos(\kappa)$.

Influence on Z is: $\Delta Z = h\ [1 - \cos(\beta + \Delta\beta)/\cos(\beta)] \approx h\ \Delta\beta \tan(\beta)$, with $\Delta\beta$ in radian.

4.2.5. Influence of ranging error ΔR

With $\Delta x = 0$; $\Delta y = \Delta R \sin(\beta)$.

The influence on X and Y is: $\Delta X = -\Delta y \sin(\kappa) = -\Delta R \sin(\beta) \sin(\kappa)$; $\Delta Y = \Delta y \cos(\kappa) = \Delta R \sin(\beta) \cos(\kappa)$.

Influence on Z is fairly constant for small to medium scan angles: $\Delta Z = -\Delta R \cos(|\beta|)$.

4.2.6. Influence of laser beam origin position errors Δx_0, Δy_0, Δz_0

$\Delta X = \Delta x_0 \cos(\kappa) - \Delta y_0 \sin(\kappa)$; $\Delta Y = \Delta x_0 \sin(\kappa) + \Delta y_0 \cos(\kappa)$; $\Delta Z = \Delta z_0$.

In the following, an example will be given using the values:
$\Delta\omega = \Delta\psi = 0.03$ deg; $\Delta\kappa = 0.04$ deg; $\Delta\beta = 0.02$ deg, $\Delta R = -5$ cm, $\Delta x_0 = \Delta y_0 = \Delta z_0 = 8$ cm.

The above values are realistic, whereby the attitude errors are based on typical values (see Table 1 in Baltsavias, 1999). The total coordinate error is the square root of the sum of the squares of the individual errors. This means that correlations between errors are ignored. However, the dependencies between the errors are small, with the exception of $\Delta\omega$ and $\Delta\beta$, which can partially cancel out. On the other hand, the height error in Table 1 is rather optimistic. The reason is that (a) flat terrain is assumed, e.g., no influence of $\Delta\kappa$, Δx_0, Δy_0 on height, and (b) the range error is assumed to be independent of flying height and scan angle. Latter is not exactly so, since larger flying height and scan angle, mean larger range (i.e., weaker recorded response), increased danger of no canopy penetration, reflections from other objects or away from the sensor, etc. Thus, we believe that, although reality is fairly complicated and other conditions that the ones assumed here can occur, the values in Table 1 are generally realistic and permit an insight into the influence of various error sources on 3D coordinate errors as well as the relation of these errors among each other.

Some conclusions from Tables 1 and 2 and Fig. 4 can be drawn:

- Ranging errors have a small influence compared to the other error sources, and influence more the height.
- ΔZ does not increase linearly with flying height and scan angle for small and medium scan angles. The reason is that the ranging error ΔR and

Table 2
Ratios of coordinate errors $\Delta X/\Delta Y/\Delta Z$ for various cases

Flying height (m)	Scan angle β (deg)	$\kappa = 0$ deg	$\kappa = 45$ deg
400	0	2.4/2.8/1	2.6/2.6/1
	−7.5	2.3/2.6/1	2.5/2.5/1
	−15	2.0/2.3/1	2.1/2.1/1
	−30	1.6/1.6/1	1.6/1.6/1
1000	0	5.6/6.8/1	6.2/6.2/1
	−7.5	4.2/5/1	4.6/4.6/1
	−15	2.9/3.3/1	3.1/3.1/1
	−30	1.8/1.7/1	1.7/1.7/1

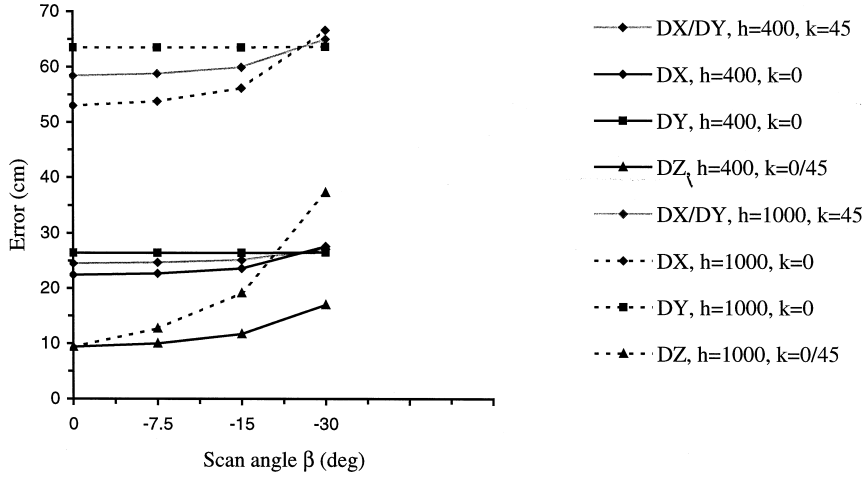

Fig. 4. Errors of 3D coordinates in relation to flying height, scan angle and κ.

position error Δz_0, which for these angles dominate the total error budget, are relatively stable with respect to flying height and scan angle. ΔZ increases substantially (and deteriorates more rapidly than ΔX and ΔY) for large scan angles and flying height. This places very high attitude accuracy requirements, if the flying height and scan angle are to be increased for higher productivity and lower costs.

- For both ΔX and ΔY and independently of scan angle and κ, a doubling of the flying height increases the error by ca. factor 2.4.
- For $\kappa = 45$ deg, an increasing scan angle has a small effect (e.g., a ca. 11% error increase by increasing β from 0 to -30 deg) for both ΔX and ΔY and independently of flying height. For $\kappa = 0$ deg, an increasing scan angle has a medium effect (e.g., a ca. 24% error increase by increasing β from 0 to -30 deg) for ΔX and independently of flying height, while ΔY does not change with scan angle. The reason is that the major error contributions to ΔX and ΔY from $\Delta\omega$, $\Delta\psi$, and $\Delta\beta$ do not change with scan angle. For $\kappa = 0$ deg, ΔY is influenced by $\Delta\beta$ and ΔR (ΔX not), while ΔX by $\Delta\kappa$ (ΔY not).
- For $\kappa = 45$ deg, the ratio $\Delta X/\Delta Y$ is 1. For $\kappa = 0$ deg, the ratio $\Delta Y/\Delta X$ is ca. 1.1–1.2, is fairly stable with respect to flying height and decreases slightly with increasing scan angle to ca. 1. For $\kappa = 90$ deg, the same would hold for the ratio $\Delta X/\Delta Y$. In other words, the error across-track is slightly larger than the error in track direction (in absolute value, especially for small scan angles and high flying height).
- The ratio of ΔX and ΔY over ΔZ is much larger (i.e., planimetry deteriorates as compared to height), the smaller the scan angle and especially the higher the flying height. This is valid independently of κ.

If the terrain is not flat, then ΔZ will increase and will approach or even exceed the planimetric error ΔXY, according to (see also Fig. 5a) $\Delta Z = \Delta XY \tan(i)$, with i the local terrain inclination.

In addition, sloped terrain will cause a ΔZ error, due to a ranging error ΔR caused by an increased rise time Δt_{rise} (see Fig. 5b). The vertical (and horizontal) spreading of the laser pulse in sloped terrain is causing a so-called time-walk. Assuming a vertical scan angle, Δt_{rise} is,

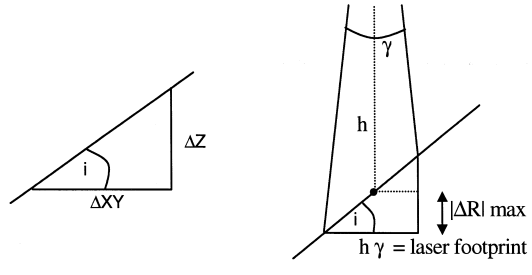

Fig. 5. (a) Relation of planimetric and height errors in case of sloped terrain. (b) Influence of sloped terrain on measured range.

$\Delta t_{rise} = 2h\gamma \tan(i)/3000$, with dt in ns, h in m and gg in mrad

In this case, the maximum absolute range error $|\Delta R|$ max will approximately be
$|\Delta R|$ max $= h\gamma\ |\tan(i)|/2$,e.g., for $i = 45$ deg, $\gamma = 1$ mrad, $h = 400$ m/1000 m: $|\Delta R|$ max = 20 cm/50 cm.

Acknowledgements

I would like to thank R. Katzenbeisser and A. Wehr for proof-reading the formulas and critical remarks.

Appendix A. Terminology and used symbols

Latin symbols

A (km^2/h)	Covered survey area
A_1 (m^2)	Area illuminated by laser beam
A_L (m)	Laser footprint diameter. Distinguish to beam diameter. The laser beam diameter is defined as the distance between diametrically opposed points in the cross-section of a circular beam where the intensity is reduced by a factor of 1/3 (0.368) of the peak level (for safety standards). The value is normally chosen at $1/e^2$ (0.135) of the peak level for manufacturing specifications.
$A_{L_{inst}}$ (m)	Instantaneous laser footprint diameter
A_r (m^2)	Area of receiving optics
A_{tar} (m^2)	Target area
B (Hz)	Bandwidth
B_{CW} (Hz)	Noise input bandwidth (CW lasers)
B_{pulse} (Hz)	Noise input bandwidth (pulse lasers)
c (km/s)	Speed of light ≈ 300,000 km/s; 1 ns corresponds to 30 cm travel distance or 15 cm range
D (cm)	Aperture of laser
D_r (m)	Diameter of receiving optics
D_{tar} (m)	Diameter of target object
d (points/m^2)	Average point density
dx_{across} (m)	Average point spacing across track (in scan direction)
$dx_{across_{inst}}$ (m)	Instantaneous average point spacing across track (in scan direction)
dx_{along} (m)	Average distance between scan lines (along track, in flight direction)
E (J)	Energy per pulse
E_r (J)	Energy received
f (Hz)	Frequency
f_{high}, f_{low}	For CW lasers employing two frequencies, the high and low frequency, corresponding to λ_{short} and λ_{long}, respectively. The low frequency is used to determine unambiguously the range, and the high one for the fine measurement.
F (kHz)	Pulse rate (pulse repetition rate, pulse repetition frequency (PRF), measurement rate)
f_{sc} (Hz)	Scan rate (number of scan lines per second)
h (m)	Average flying height over ground
i (deg)	Inclination angle of local planar terrain surface with respect to horizontal plane
L (km)	Longest dimension of rectangular survey area
M	Atmospheric transmission. Values from 0 to 1, depending on the amount of absorption and scattering of light for the given atmospheric conditions
N	Number of points per scan line, and for fiber scanners number of fibers of the scan line
n	Number of flying strips necessary to cover rectangular area to be surveyed
P (W)	Laser power
P_{av} (W)	Average power (applies to pulse and CW lasers)
P_{peak} (W)	Peak power (applies only to pulse lasers)

P_T (W)	Transmitted power
q (%)	Overlap between strips
Q_{across} (%)	Oversampling/undersampling across track
Q_{along} (%)	Oversampling/undersampling along track
R (m)	Range (distance between sensor and object)
ΔR (cm)	Range resolution
R_{min} (m)	Minimum object separation, i.e., minimum distance between two objects so that their echoes, within one pulse, can be separated (important only for systems that can record more than one echo per pulse)
R_{max} (m)	Maximum unambiguous range
s (m)	Travel distance of the aircraft between sending and receiving pulse
S (MBytes)	Data size (after basic preprocessing, i.e., delivered raw laser points in local coordinate system)
S/N	Signal to noise ratio
SW (m)	Swath width
T (s)	Period
T_f (h)	Netto flying time (netto time—the time during which data acquisition occurs)
T_s (h)	Netto flying time per strip
t (ns)	Time between sending and receiving a pulse (or echo)
Δt (ns)	Resolution of time measurement
t_p (ns)	Pulse duration or pulse width. Duration of a laser pulse, usually measured as the time interval between the half-peak-power points on the leading and trailing edges of the pulse (called also FWHM, full width half maximum).
t_{rise} (ns)	Rise time of pulse. Time required for the optical output to rise from 10% to 90% of its maximum value.
t_{min} (ns)	Minimum time difference between two received echoes, in order to be separable (t_{min} assumed here to be equal to the pulse duration t_p; others use $t_{min} = t_p/2$ or $t_{min} = t_p + t_{rise}$)
t_{sc} (s)	Period to scan a line $= 1/f_{sc}$
v (m/s)	Flying speed over ground
W (km)	Smallest dimension of rectangular survey area

Greek symbols

γ (mrad)	Laser beam divergence (IFOV)
θ (deg)	Laser scan angle (FOV)
θ_{inst} (deg)	Instantaneous scan angle; θ_{inst} takes values in the range $[0, +\theta/2]$
$\dot{\theta}$ (deg/s)	Angular scan speed
$\dot{\theta}_{inst}$ (deg/s)	Instantaneous angular scan speed
λ (nm)	Wavelength of laser
λ_{long}, λ_{short} (nm)	Long and short wavelengths corresponding to the low and high frequencies of a CW laser
ν	Laser frequency
ρ	Reflectivity of target. Values from 0 to 1, or 0% to 100%. Reflectivity depends on target colour and composition and laser wavelength. Diffuse surfaces generally vary from 3% to 95% reflectivity.
σ_R (m)	Ranging precision
ϕ (rad)	Phase (for CW lasers)
$\Delta\phi$ (rad)	Phase resolution (for CW lasers)
Φ_{tar} (W/m^2)	Power density within an illuminated target

References

Baltsavias, E.P., 1999. Airborne laser scanning: existing systems and firms and other resources. ISPRS J. Photogr. Rem. Sensing 54 (2/3), 164–198, this issue.

Gardner, C.S., 1992. Ranging performance of satellite laser altimeters. IEEE Trans. Geosci. Rem. Sensing 30 (5), 1061–1072.

Wehr, A., Lohr, U., 1999. Airborne laser scanning—an introduction and overview. ISPRS J. Photogr. Rem. Sensing 54 (2/3), 68–82, this issue.